Développement d'un modèle pour l'environnement urbain basé sur l'approche RANS transitoire

Developing a model for Urban Environment based on transient RANS approach

Hamidreza Mohammadpour[1,2*], Stephanie Giroux-Julien[1], Victoria Timchenko[2], Auline Rodler[3], Eric Peyrol[1]

[1] LAGEPP, UMR 5007, Université Claude Bernard Lyon 1
43 Bd du 11 Novembre 1918, 69100 Villeurbanne, France
[2] University of New South Wales
Sydney NSW 2033, Australia
[3] CEREMA Equipe, BPE
*(hamidreza.mohammadpour@univ-lyon1.fr)

Résumé

La température de l'air ambiant dans une ville est un paramètre critique pour le confort thermique urbain. Elle influence également fortement les besoins en énergie pour le refroidissement et le chauffage des bâtiments. Les propriétés thermiques et radiatives de ces surfaces affectent la température de l'air ambiant. L'utilisation de revêtements spécialement conçus pour l'ensemble de ces surfaces peut donc être un moyen efficace de contrôler cet environnement urbain local et la température des rues canyon. L'objectif de cet article est de décrire le modèle développé, adapté à une utilisation dans les études thermiques urbaines, et de montrer la précision des résultats en les comparant à des données issues de campagnes expérimentales en milieu urbain. Les résultats sont également confrontés aux résultats issus de simulations basées sur des modèles. Le solveur en volumes finis du logiciel ANSYS/FLUENT 22 est utilisé pour résoudre les équations de Navier-Stokes moyennées instationnaires (modèle URANS).

Abstract

The ambient air temperature in a city is a critical parameter for thermal comfort. It also strongly influences energy needs for cooling and heating. Thermal and radiative parameters of these surfaces can affect urban ambient air temperature and street canyon temperature. So, using specially designed pavements on buildings and surfaces on the streets can be an effective way to control the local urban environment. The aim of this paper is to describe the developed model, suitable to use in urban thermal studies, and to show the accuracy of the result by comparing them to real data that have been published from data gathering campaigns. Also, results are compared with other models to measure the accuracy of this model against others. Finite Volume solver in ANSYS/FLUENT 22. software is used to solve unsteady Reynolds Averaged Navier Stokes (URANS) equations.

Nomenclature

A	Area of surface i, m^2	K_t	Turbulence conductivity, $W.m^{-1}.K^{-1}$
C	Volumetric heat capacity, $J.m^{-3}.K^{-1}$	N	Number of surfaces
C_p	Specific heat capacity, $J.kg^{-1}.K^{-1}$	P	Pressure, Pa
E	Total energy, J	$q_{in,i}$	Energy flux into surface i
$F_{i,j}$	View factor between surfaces i and j	$q_{out,i}$	Energy flux leaving surface i
G_b	Turbulence generation from buoyancy, $J.m^{-3}.s^{-1}$	S	Source terms

https://doi.org/10.25855/SFT2025-152

G_k	Turbulence generation from mean velocity gradients	T	Temperature, K
h	Enthalpy, J	v	Velocity, $m.s^{-1}$
k	Turbulence kinetic energy, $J.kg^{-1}$	Z_H	Building height, m
K_{eff}	Effective conductivity, $W.m^{-1}.K^{-1}$		
Greek symbols			
$\alpha_{i,j}$	Visibility indicator of surface i and j	μ	Viscosity, $Kg.m^{-1}.s^{-1}$
α_{IR}	Infrared absorptivity	μ_t	Turbulence viscosity, $kg.m^{-1}.s^{-1}$
α_{VS}	Visible absorptivity	ρ_i	Reflectivity
$\delta_{i,j}$	Kronecker delta	ρ	Density, $kg.m^{-3}$
ε	Turbulence dissipation rate	σ	Boltzmann constant, $W.m^{-2}.K^{-4}$
ε_i	Emissivity of surface i	τ	Viscous shear, $kg.m^{-1}.s^{-2}$
θ_i			

1. Introduction

With the increasing urban population all across the globe, cities are expanding rapidly, resulting in significant environmental changes in urban areas [1-3]. Furthermore, urban expansion often replaces vegetated and natural landscapes with buildings, roads, and other infrastructure. surfaces such as rooftops and pavements typically have lower albedo values, causing them to absorb and retain more solar energy. This leads to an increase in surface temperature which has a significant impact on air temperature, particularly within the urban canopy layer [4-6] which plays a crucial role in the thermal dynamics of cities. There are two main strategies for Urban Heat Island mitigation. First, the development of green infrastructures and second, the use of sustainable materials with improved thermal properties to reduce surface temperatures [7]. These materials, often referred to as "cool materials", are specifically designed for applications such as street pavements and building coatings. Previous studies have demonstrated that cool materials applied to street pavements and building walls can significantly reduce surface temperature in urban areas by influencing the thermal energy balance. They achieve this through mechanisms such as reducing thermal energy storage in the material and underlying soil, decreasing absorbed solar energy, and enhancing emitted radiation [5].

As mentioned before, surface albedo is one of the critical parameters influencing surface and urban ambient temperature. Urban surfaces can be categorized into four main parts, natural surfaces, street surfaces, building roofs, and building walls. It is therefore essential to evaluate the impact of the albedo of these three components on street canyon temperatures and the Urban Heat Island (UHI) effect simultaneously. Studying this parameter on real experimental cases in cities is costly, time-consuming, and almost impossible to execute. Hence, two alternative approaches are commonly employed. First, making scaled models and conducting experimental studies on them, like the study by Lu et al. in a suburb of Guangzhou, China [8]. Second, using computational analysis which can be used in a very extensive range of studies and it is much less costly. Consequently, most investigations in this field rely on computational modeling. Numerous studies have investigated the impact of roof surface albedo on urban ambient temperature using computational techniques such as meso-scale and Computational Fluid Dynamics (CFD) models. While meso-scale models are suitable for large-scale analyses, they are very coarse and can't capture and calculate all the details on heat transfer, radiation and air flow between building walls, roofs, streets and street canyons. In contrast, CFD models can simulate all of these interactions

more accurately in fine grids. For this reason, CFD models have been utilized to study the cooling effects of using cool materials in urban environments [9-12].

While these studies provide solid insights into the thermal effect of cool materials on cities, only two specifically examine the effect of cool material on urban environment (ambient temperature) in addition to surface temperature [9, 12]. Further research is therefore required to investigate the effect of using cool materials in cities on urban environment.

In this paper, the development of a CFD model using Ansys Fluent 22.R2 software is described and the accuracy of this model is presented. In future works this model will be used to simulate the urban environment and the thermal effect of cool materials on street pavements, building roof and building walls on surface and ambient temperature will be studied. The contents of this paper are organized as follow. In sections 2, details of numerical model and different cases simulated in this paper are described. Section 3 is dedicated to explaining radiation model and governing equations. Section 4 presents the validation of numerical model, and an analysis of the simulation results. The overall conclusion of the study is presented in section 5.

2. Model description

Turbulent airflow, along with conduction, convection and radiation heat transfer, is simulated in ANSYS Fluent 22.R2. The geometry details are shown in Figure 1. Buildings are represented as cubes, and the domain contains of nine cubes arranged in a 3×3 matrix, all with identical geometry place over a surface modeled as street surface.

The building walls consist of three layers, the street surface includes two underground soil layers in addition to the surface layer that represents the street. All outer boundaries of the building walls and the street surface have wall (no slip) boundary condition for velocity and radiation plus convection for thermal boundary condition. The inner boundaries of building walls, as well as the deep soil boundary located beneath the soil layers, are set to constant temperature boundary condition. The details and material properties of the layers are listed in section 4.

The airflow (wind) enters the computational domain from right-side boundary, which is set to inlet boundary condition. The wind speed and temperature are determined in this boundary from in site data measured in [13], and an exponential velocity profile is applied. The top boundary is set to zero shear boundary condition and the temperature is constant in this boundary, this boundary is considered as sky and the temperature is set to sky temperature since it is important to consider the long-wave radiation between sky and surfaces of domain. This temperature is calculated using formula presented by Walton [13, 14]. Solar radiation is added to the model using solar ray tracing model which provided in Ansys Fluent software. Heat fluxes calculated from this model are coupled to Ansys Fluent via a source term in boundary condition equation of surfaces.

The simulations in this study are time-dependent and are conducted over a full day, so sun position and sun radiation parameters change over time. Radiation within the geometry is modeled using the Surface-to-Surface (S2S) radiation model, provided in ANSYS Fluent software, and resulting heat fluxes are added to energy equation via source term. Energy and Navier-stokes equations are solved using Finite Volume Method (FVM). The details of the radiation model and governing equations are explained in following sections.

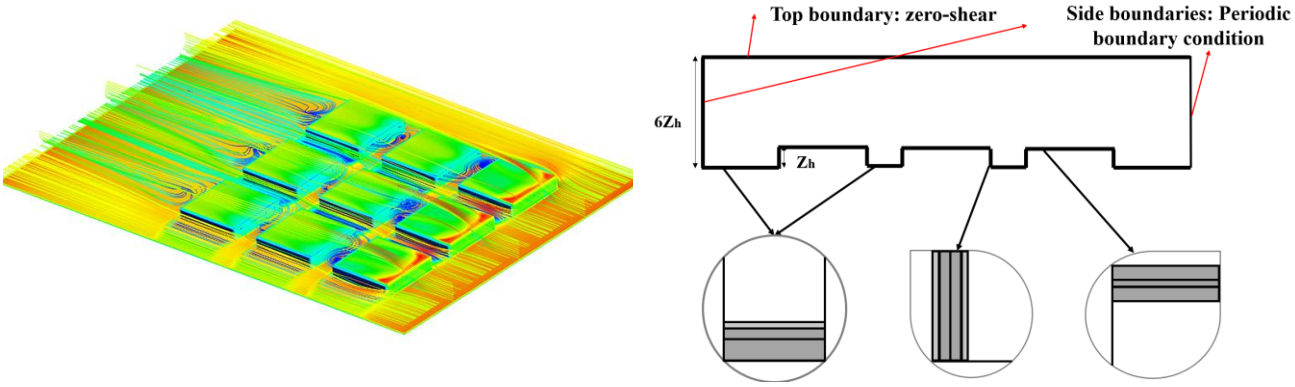

Figure 1: Left: Computational domain with surface temperature and stream lines. Right: Cross section of the computational domain

3. Governing equations

This section introduces the governing equations, including the continuity and momentum (Navier-stokes) equations, the surface-to-surface (S2S) radiation model and the energy equation.

3.1. Continuity equation, Reynolds-averaged Navier Stokes equation and Turbulence model

Considering the urban flow characteristics and wind velocity in our simulations, the Mach number is relatively low and the airflow can be treated as incompressible. The continuity equation for incompressible flows has the following form:

$$\frac{\partial u_i}{\partial x_i} = 0 \tag{1}$$

Also, Reynolds-averaged Navier Stokes equation is the following:

$$\frac{\partial}{\partial t}\left(\rho u_i\right) + \frac{\partial}{\partial x_j}\left(\rho u_i u_j\right) = -\frac{\partial P}{\partial x_i} + \frac{\partial}{\partial x_j}\left[\mu\left(\frac{\partial u_i}{\partial x_i} + \frac{\partial u_j}{\partial x_i} - \frac{2}{3}\delta_j \frac{\partial u_l}{\partial x_l}\right)\right] + \frac{\partial}{\partial x_j}\left(-\rho\overline{u_i' u_j'}\right) \tag{2}$$

The last term in this equation represents the Reynolds stress, which must be modeled to close equation (2). A common method for this purpose is to use Boussinesq hypothesis, expressed in equation (3) and use turbulence models to compute it.

$$-\rho\overline{u_i' u_j'} = \mu_t\left(\frac{\partial u_i}{\partial x_j} + \frac{\partial u_j}{\partial x_i}\right) - \frac{2}{3}\left(\rho k + \mu_t \frac{\partial u_k}{\partial x_k}\right)\delta_{ij} \tag{3}$$

The k-ε model has been employed in this work as the turbulence model. This model introduces two additional transport equations: one for the turbulence kinetic energy (k) (equation (4)) and another for the turbulence dissipation rate (ε) (equation (5)), to close the equation (2). Using these two parameters, the turbulence viscosity (μ_t) can be calculated with equation (6).

$$\frac{\partial}{\partial t}\left(\rho k\right) + \frac{\partial}{\partial x_i}\left(\rho k u_i\right) = \frac{\partial}{\partial x_j}\left[\left(\mu + \frac{\mu_t}{\sigma_k}\right)\frac{\partial k}{\partial x_j}\right] + G_k + G_b - \rho\varepsilon + S_k \tag{4}$$

$$\frac{\partial}{\partial t}(\rho\varepsilon)+\frac{\partial}{\partial x_i}(\rho\varepsilon u_i)=\frac{\partial}{\partial x_j}\left[\left(\mu+\frac{\mu_t}{\sigma_\varepsilon}\right)\frac{\partial\varepsilon}{\partial x_j}\right]+C_{1\varepsilon}\frac{\varepsilon}{k}(G_k+C_{3\varepsilon}G_b)-C_{2\varepsilon}\rho\frac{\varepsilon^2}{k}+S_\varepsilon \tag{5}$$

$$\mu_t=\rho C_\mu\frac{k^2}{\varepsilon} \tag{6}$$

In this model, $C_{1\varepsilon}$, $C_{2\varepsilon}$, C_μ, σ_k and σ_ε are all constants and have the following values:

$C_{1\varepsilon}=1.44$ $C_{2\varepsilon}=1.92$ $C_\mu=0.09$ $\sigma_k=1$ $\sigma_\varepsilon=1.3$

Additionally, G_k represents the generation of turbulence kinetic energy due to mean velocity gradients, while G_b represents the generation of turbulence kinetic energy due to buoyancy.

3.2. Surface-to-Surface (S2S) radiation model and Energy equations

Energy fluxes leave each surface of the geometry in the form emitted radiation as well as the reflection of radiation emitted by other surfaces. The energy flux leaving the surface "i" can be expressed as follows.

$$q_{out,i}=\varepsilon_i\sigma T_i^4+\rho_i q_{in,i} \tag{7}$$

The energy fluxes incident on surface "i" from another surface depend on whether these two surfaces "see" each other or not. This interaction is quantified by calculating the view factor between the two surfaces. The view factor between two surfaces can be calculated as:

$$F_{ij}=\frac{1}{A_i}\int_{A_i}\int_{A_j}\frac{\cos\theta_i\cos\theta_j}{\pi r^2}\alpha_{ij}dA_i dA_j \tag{8}$$

If dA_i is visible to dA_j, $\alpha_{ij}=1$ and if it is not visible $\alpha_{ij}=0$. The incident energy flux to surface "i" can now be calculated using equation (9). In this equation, N is the number of surfaces surrounding surface "i" in the geometry.

$$A_i q_{in,i}=\sum_{j=1}^{N}A_j q_{out,j}F_{ji} \tag{9}$$

Using view factor reciprocity relationship which is:

$$A_j F_{ji}=A_i F_{ij} \tag{10}$$

Equation (9) and therefore equation (7) can respectively written as:

$$q_{in,i}=\sum_{j=1}^{N}q_{out,j}F_{ij} \tag{11}$$

$$q_{out,i}=\varepsilon_i\sigma T_i^4+\rho_i\sum_{j=1}^{N}q_{out,j}F_{ij} \tag{12}$$

This represents N equations, which can recast into matrix form and solved.

The energy equation in the fluid regions has the following form:

$$\frac{\partial}{\partial t}(\rho E) + \nabla.\left(\vec{v}\,(\rho E + P)\right) = \nabla.\left(k_{eff}\,\nabla T + \left(\bar{\bar{\tau}}_{eff}.\vec{v}\right)\right) \tag{13}$$

In this equation:

$$E = h - \frac{P}{\rho} + \frac{v^2}{2} \tag{14}$$

$$h = \int_{T_{ref}}^{T} c_p dT \tag{15}$$

Also, K_{eff} is effective conductivity and it's consisted of two parts:

$$K_{eff} = K + K_t \tag{16}$$

K_t is turbulent conductivity, defined according to the turbulence model.

The energy equation in solid regions is:

$$\frac{\partial}{\partial t}(\rho h) = \nabla.(k\,\nabla T) \tag{17}$$

The enthalpy (h) can be calculated using equation (15). The calculated heat fluxes in the radiation model, are added to the energy equation as source term in boundary condition equation of surfaces.

4. Validation

The time variation of the roof surface temperature is validated against real site measurements conducted at the Vancouver lite industrial site [13]. Furthermore, the results are compared with three-dimensional energy balance model (TUF3D) and the Town Energy Balance model (TEB) presented in [14]. The data gathering campaign was carried out in August of 1992. The Vancouver lite industrial site consists of one to three-story buildings, and the area has distinct lack of vegetation. The wind speed varied throughout the day during the data collection campaign, and this diurnal variation is presented in Figure 2. Input parameters, including material properties, geometric parameters, and initial values, are same as reported in Table 2 of [14]. Radiative parameters, and also parameters related to the mesh, and the solver are listed in Table 1. It is worthy to mention that the Reynolds number of our simulations is around 4500, and also convergence criteria is residuals. Residuals thresholds for convergence for Continuity, Momentum and turbulence parameters equations is 1×10^{-3} and for energy equation is 1×10^{-6}. The residuals in the simulations conducted in this study are smaller than the specified thresholds, ensuring that convergence has been achieved.

As shown in Figure 3, the results from this work have a good agreement with real site measurements. The maximum roof surface temperature (44.15˚C) is close to the maximum temperature measured on-site (44.41˚C–50.02˚C). Furthermore, the time of day at which this maximum temperature occurs (13:30h) is also close with the on-site data (12:30h). This shows the accuracy of the model developed in this study using ANSYS Fluent software and its reliability for future applications in studying the thermal effects of various cool pavements on urban environments. However, there is a difference between the results of this model and those obtained from the TUF3D and TEB models. Specifically, before sunrise, when longwave radiation is the dominant heat transfer mechanism, the scope of the temperature variation predicted by this model

differs from that of the TUF3D and TEB models. This discrepancy arises from differences in how the surface-to-surface radiation model used in this study and the radiation models in TUF3D and TEB handle longwave radiation. Additionally, the input material properties of surface for longwave and shortwave radiation are needed in these models. For instance, in the surface-to-surface radiation model there is no longwave and shortwave emissivity needed as material properties for surfaces; instead, parameters such as direct infrared absorptivity, and direct visible absorptivity are required.

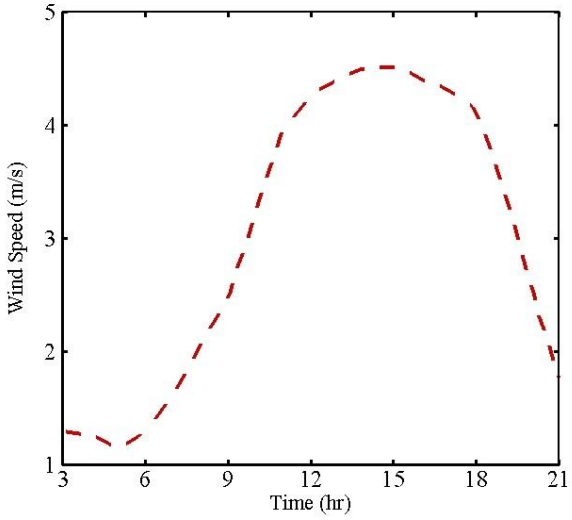

Figure 2: Wind speed during data collection [14]

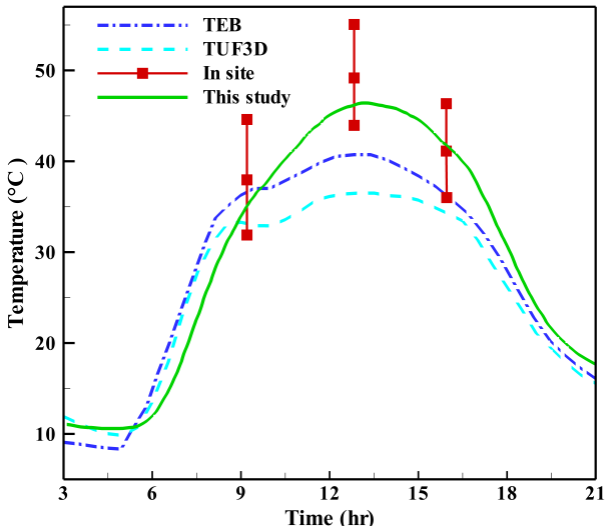

Figure 3: Validation of average roof surface temperature

Parameter	Value
Radiative	
α_{IR}	0.88
α_{VS}	0.92
Geometric	
Z_H, *m*	5.79
Street Width, m	11.58
Building Length, m	28.95
Mesh number	36000
Solver	
Time step, s	30

Table 1: Parameters employed in the model

5. Conclusion

As described in previous section, the model developed in this work using ANSYS Fluent software has a good accuracy and it's reliable to use in future studies on thermal effect of roof surface material on urban environment. This model accurately predicts the trends in durational

changes of average roof surface temperature in addition to maximum temperature. The calculated roof surface temperatures are within the uncertainty range of the temperature sensors used in the experimental study conducted by Voogt and Grimmond (2000) [13].

Acknowledgment

Co-funded by the European Union under the Marie Skłodowska-Curie Grant Agreement No 101081465 (AUFRANDE). Views and opinions expressed are however those of the author(s) only and do not necessarily reflect those of the European Union or the Research Executive Agency. Neither the European Union nor the Research Executive Agency can be held responsible for them.

References

[1] B. Güneralp, M. Reba, B.U. Hales, E.A. Wentz, K.C. Seto, Trends in urban land expansion, density, and land transitions from 1970 to 2010: A global synthesis, Environmental Research Letters 15(4) (2020) 044015.
[2] J. Gibson, G. Boe-Gibson, G. Stichbury, Urban land expansion in India 1992–2012, Food Policy 56 (2015) 100-113.
[3] W. Fei, S. Zhao, Urban land expansion in China's six megacities from 1978 to 2015, Science of the Total Environment 664 (2019) 60-71.
[4] A.T. Hayes, Z. Jandaghian, M.A. Lacasse, A. Gaur, H. Lu, A. Laouadi, H. Ge, L. Wang, Nature-based solutions (nbss) to mitigate urban heat island (UHI) effects in Canadian cities, Buildings 12(7) (2022) 925.
[5] S. Kappou, M. Souliotis, S. Papaefthimiou, G. Panaras, J.A. Paravantis, E. Michalena, J.M. Hills, A.P. Vouros, A. Ntymenou, G. Mihalakakou, Cool pavements: State of the art and new technologies, Sustainability 14(9) (2022) 5159.
[6] S. Ren, C. Stroud, Impacts of urban canyon aspect ratio and roof albedo on heat fluxes and temperatures in four urban centers, Urban Climate 44 (2022) 101189.
[7] A.M.M. Irfeey, H.-W. Chau, M.M.F. Sumaiya, C.Y. Wai, N. Muttil, E. Jamei, Sustainable mitigation strategies for urban heat island effects in urban areas, Sustainability 15(14) (2023) 10767.
[8] M. Lu, L. Zeng, Q. Li, J. Hang, J. Hua, X. Wang, W. Wang, Quantifying cooling benefits of cool roofs and walls applied in building clusters by scaled outdoor experiments, Sustainable Cities and Society 97 (2023) 104741.
[9] N. Nazarian, J. Kleissl, CFD simulation of an idealized urban environment: Thermal effects of geometrical characteristics and surface materials, Urban Climate 12 (2015) 141-159.
[10] F. Xu, J. Zhang, Z. Gao, The effect of building surface cool and super cool materials on microclimate in typical residential neighborhoods in Nanjing, Sustainable Cities and Society 98 (2023) 104838.
[11] Z. Zhu, D. Zhou, Y. Wang, D. Ma, X. Meng, Assessment of urban surface and canopy cooling strategies in high-rise residential communities, Journal of Cleaner Production 288 (2021) 125599.
[12] M. Hadavi, H. Pasdarshahri, Impacts of urban buildings on microclimate and cooling systems efficiency: Coupled CFD and BES simulations, Sustainable Cities and Society 67 (2021) 102740.
[13] J.A. Voogt, C. Grimmond, Modeling surface sensible heat flux using surface radiative temperatures in a simple urban area, Journal of Applied Meteorology 39(10) (2000) 1679-1699.
[14] E.S. Krayenhoff, J.A. Voogt, A microscale three-dimensional urban energy balance model for studying surface temperatures, Boundary-Layer Meteorology 123 (2007) 433-461.